Two-Dimensional Microrheology of Freely Suspended Liquid Crystal Films

A. Eremin, S. Baumgarten, K. Harth, R. Stannarius, Z. H. Nguyen, A. Goldfain, C. S. Park, J. E. Maclennan, M. A. Glaser, and N. A. Clark

Phys. Rev. Lett. **107**, 268301 — Published 22 December 2011

DOI: 10.1103/PhysRevLett.107.268301

Two-dimensional microrheology of freely-suspended liquid crystal films

A. Eremin, S. Baumgarten, K. Harth, and R. Stannarius
Otto-von-Guericke Universität Magdeburg, Institute for Experimental Physics, D-39016 Magdeburg, Germany

Z. H. Nguyen, A. Goldfain, C. S. Park, J. E. Maclennan, M. A. Glaser, and N. A. Clark
Department of Physics, and the Liquid Crystal Materials Research Center, University of Colorado, Boulder, CO, 80309, USA

Smectic liquid crystals form freely-suspended, fluid films of highly uniform structure and thickness, making them ideal systems for studies of hydrodynamics in two dimensions. We have measured particle mobility and shear viscosity by direct observation of the gravitational drift of silica spheres and smectic islands included in these fluid membranes. In thick films, we observe a hydrodynamic regime dominated by lateral confinement effects, with the mobility of the inclusion determined predominantly by coupling of the fluid flow to the fixed boundaries of the film. In thin films, the mobility of inclusions is governed primarily by coupling of the fluid to the surrounding air, as predicted by Saffman-Delbrück theory.

PACS numbers: 83.80.Xz, 47.57.Lj, 68.15.+e, 83.50.Ax

Flow phenomena in restricted geometries have been studied in a variety of different physical, chemical and biological systems, including the motion of proteins in lipid membranes [1, 2] and studies of submicrometer-sized functional lipid domains (lipid rafts) on cell membranes [3, 4]. Most rheological investigations of membranes have been made by observing Brownian motion in flat lipid membranes and spherical vesicles [3, 5, 6] as well as in liquid crystal films [7, 8], with the mobility of the inclusions calculated from the diffusion coefficient by means of the Einstein relation. This approach requires a model describing the relation between the mobility and such physical parameters as the inclusion size and the viscosities of the membrane and the surrounding fluid. Theory predicts specific hydrodynamic regimes in two dimensions (2D) [2, 9] but direct experimental study of these regimes is complicated by the difficulty of finding a 2D fluid whose relevant physical properties can be varied over a wide range. Smectic liquid crystals are particularly well suited for measuring mobilities in 2D because they form homogeneous, freely-suspended films that are quantized in thickness (they have an adjustable, integer number of smectic layers N) and are stable for many hours [10]. In this paper, we explore experimentally a variety of 2D hydrodynamic regimes and test existing theory using a direct "falling ball" rheology technique in fluid smectic films.

The relationship between the viscosity and the mobility in 2D fluid membranes is fundamentally different from that in 3D fluids. In particular, the translational mobility b (the ratio of the relative velocity v of an inclusion to the force F acting on it) diverges in a hypothetical infinite membrane in vacuum (the Stokes paradox). A full hydrodynamic description of the translational motion of an inclusion in a fluid membrane of radius R developed by Saffman and Delbrück (SD) [1, 2] shows however that a well-defined mobility is expected in practice if one considers that real membranes are finite and are typically immersed in another fluid with non-negligible viscosity η'. The ratio of the shear viscosity of the membrane to that of the surrounding fluid defines a viscous length scale, the Saffman length $\ell_S = \eta h/2\eta'$, where h is the thickness and η the viscosity of the membrane. Several dynamic regimes are predicted to occur in 2D, depending on the magnitude of ℓ_S. In the SD regime, where the size of the membrane $R \gg \ell_S$, the mobility of the inclusion is independent of film size, being determined by viscous coupling of the inclusion and the film through the surrounding fluid and given by the expression

$$b = \frac{1}{4\pi\eta h}\Big(\ln\frac{2\ell_S}{a} - \gamma\Big)\,, \tag{1}$$

where a is the radius of the inclusion and γ is the Euler constant [1, 2]. This expression is valid when the reduced inclusion radius $\varepsilon = a/\ell_S \ll 1$ and even when the inclusion protrudes from the membrane. The SD model has been extended by Hughes, Pailthorpe and White (HPW) to the case of arbitrarily large ε [9].

When the size of the system $R \ll \ell_S$, finite size effects are more important than air-film coupling and the mobility depends on the ratio of the membrane size to that of the inclusion. For a circular domain with $R \gg a$, an approximate expression for the mobility in this regime was given by Saffman [2] as

$$b = \frac{1}{4\pi\eta h}\Big(\ln\frac{R}{a} - \frac{1}{2}\Big)\,. \tag{2}$$

For an infinitely long, rectangular membrane of finite width W, we assume that the mobility of an embedded particle may be described in a similar way by

$$b = \frac{1}{4\pi\eta h}\Big(\ln\frac{W}{2a} + c\Big)\,. \tag{3}$$

Numerical solution of the 2D Navier-Stokes equations for this geometry neglecting the viscosity of the surrounding air yields sample particle mobilities from which we determine the geometrical fit parameter in Eq. 3 to be $c = -0.88 \pm 0.02$. This empirical relation is valid over a wide range of scaled widths, including the experimentally probed range of $1 \lesssim W/a \lesssim 200$.

The fluid membranes in our study are planar, freely-suspended films of smectic-A liquid crystal (LC) inclined from the horizontal. Since the film thickness can be adjusted from a few nm to a few micrometers, the Saffman length is easily varied over several orders of magnitude, and different contributions to the dynamics, such as confinement by the outer boundaries and coupling to the viscous outer fluid, can be distinguished and systematically studied. We have measured the translational mobility of both solid silica beads and of smectic islands, which are circular regions with additional smectic layers, in films of 8CB (4-*n*-octyl-4-cyanobiphenyl, Sigma-Aldridge), a smectic-A liquid crystal at room temperature.

Small silica spheres embedded in the LC were observed drifting under gravity down inclined rectangular films (Fig. 1a). The films were drawn across an adjustable metal frame usually 10×4 mm^2 in size, although in some experiments the width was reduced to as little as 1.9 mm. The motion of the beads was observed through an optical microscope, with both the film and the microscope tilted by an angle δ (Fig. 1b). The film thickness was determined to within 10 nm by visible light interferometry. The beads (with radii 5 μm $< a <$ 25 μm) were dropped from the tip of a thin glass fiber positioned about 1 mm above the film. Once a bead touches the film, it becomes immersed very quickly (within 100 ms). We measured the steady-state drift of the bead using a high-speed video camera (Photron Fastcam-Ultima APX) at frame rates up to 2000 fps.

The bead is pulled down the film by gravity, the effect of which can be tuned by changing the inclination of the film. The bead velocity v is governed by the balance between the gravitational force and viscous drag from the film and the surrounding air. Assuming that the viscosity of air at room temperature is $\eta' \approx 1.85 \cdot 10^{-5}$ Pa $\cdot$ s [11] and that of the liquid crystal $\eta \approx 0.05$ Pa$\cdot$s [12], we find that the Reynolds number for 10 µm beads is about 0.001 in LC and 0.003 in air. This means we can use the force balance equation for laminar flow

$$m\dot{v} + \frac{1}{b'}hv - mg\sin\delta = 0\ , \qquad (4)$$

where m is the mass of the inclusion, h is the thickness of the LC film, and $b' = bh$ is the scaled mobility of the inclusion in the film. A typical bead of radius 10.8 µm deposited on a film tilted by 13° reaches its terminal velocity v_∞ of a few millimeters per second after a brief transient time of the order of $\tau = v_\infty/g\sin\delta$, which is less than a millisecond. The effects of buoyancy are negligible.

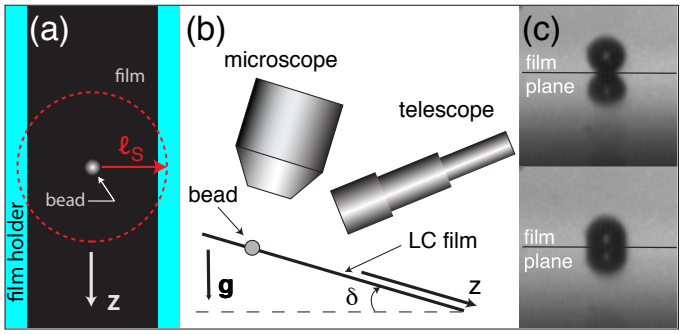

FIG. 1: Experimental setup. (a,b) A silica bead embedded in a smectic film drifts down the film under the influence of gravity g. The film is inclined from the horizontal by an angle δ and the bead is observed using a reflected light microscope. Smectic islands were studied in similar fashion. When the Saffman length ℓ_S is comparable to or exceeds the film width, the hydrodynamics are dominated by confinement effects. (c) Snapshots of a bead ($a \sim 15$ µm) shortly before contacting the LC film (top) and once immersed in the film (bottom), obtained using a telescope slightly inclined to the film plane.

The flow field in the film can be visualized using small tracer particles dispersed on the film surface. The flow pattern is characterized by rotatory motion of the fluid in the co-moving reference frame of the bead, the streamlines being circular in appearance as indicated in Fig. 2a. The fluid velocity component v_z in the direction of bead motion varies non-monotonically along x, with the fluid near the bead being dragged downward and that further away flowing back uphill (Figs. 2a and b). The extent of the fluid region involved in the flow is much larger than it would be in 3D, the flow field showing only a slow decay with distance from the bead. The measured transverse flow profile matches the fluid velocities obtained by solving the 2D Navier-Stokes equations, as shown in Fig. 2b.

We measured the terminal velocities of beads with different radii drifting down films with different widths and thicknesses. The scaled mobility b', derived from v_∞ using Eq. 4 and plotted versus $\varepsilon = a/\ell_S$ in Fig. 3, shows two regimes: one with only weak dependence of b' on ε (when $\varepsilon \lesssim 0.05$), and the other where b' varies strongly with ε (when $\varepsilon \gtrsim 0.05$). In the latter regime (the right side of Fig. 3), the bead mobilities are close to the predictions of SD theory, confirming that air-film coupling is the main dissipation pathway when $\ell_S < W$, and the data merge smoothly into the island mobilities discussed below.

The region with small ε (the left side of Fig. 3) coincides with the regime where the Saffman length is greater than (or at least comparable to) the width of the film ($2 \lesssim \ell_S \lesssim 10$ mm). The measured bead mobilities fall well below the predictions of SD theory here because the dynamics are dominated by confinement, i.e., the proxim-

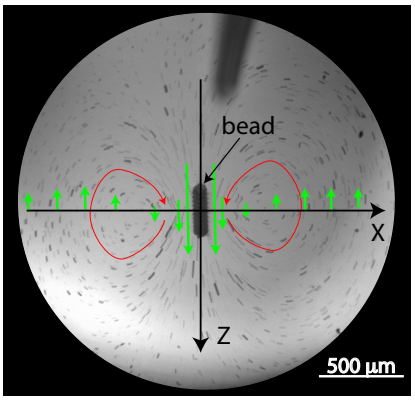

(a)

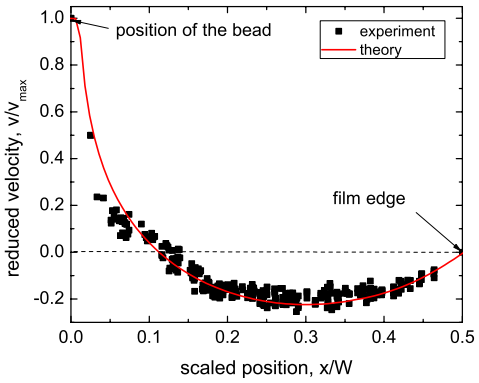

(b)

FIG. 2: (a) Composite stroboscopic image of a bead of radius 44 µm moving with terminal velocity 2300 µm/s down a rectangular 8CB film 2.5 mm wide, 400 nm thick, and tilted by 13°. The streamlines, which are visualized using tracer particles, are indicated as red loops, with the flow field on either side of the bead sketched with green arrows. The blurred shadow at top is from the glass fiber used to deposit the bead. (b) Film flow velocity profile $v_z(x)$ measured from the center of the bead to the edge of the film, normalized by the bead velocity. The theoretical curve is obtained from a finite-element solution of the Navier-Stokes equations.

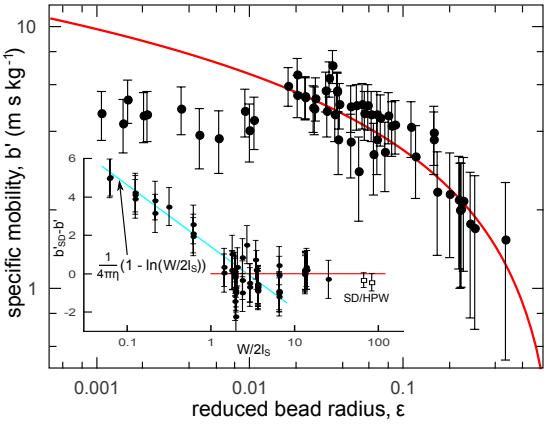

FIG. 3: Scaled mobility of beads as a function of reduced radius in films with thicknesses ranging from 100 nm to 22 µm and of width $W = 4.0$ mm, inclined by $\delta = 14°$. When the Saffman length $\ell_S < W$ (right), the mobility is determined by air-film coupling and is reproduced by Eq. 1 (red curve). When $\ell_S > W$ (left), the response of the fluid is dominated by confinement effects. The inset shows the difference between the measured bead mobilities and SD/HPW theory as a function of $W/2\ell_S$. The blue and red lines show theoretical predictions in the confinement and SD regimes respectively. The bead mobilities merge smoothly with the beginning of the island data (open symbols).

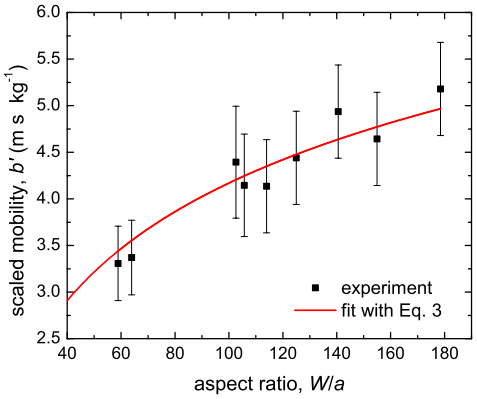

FIG. 4: Scaled mobility of embedded beads vs. the ratio of film width to bead radius for rectangular films of thickness 875± 10 nm tilted by 14°. The film width W was varied from 4 mm to about 1.9 mm. The blue curve is a fit to Eq. 3.

ity of the fixed boundaries becomes important. Although b' shows little variation with h in this regime, there is a strong dependence on the ratio W/a, as illustrated in Fig. 4. The mobility in this regime is well described by Eq. 3, a fit to the experimental data yielding a value of the shear viscosity of 8CB $\eta = 0.057$ Pa·s, in good agreement with values reported in the literature [12]. A crossover from the SD regime to confinement-dominated behavior would be expected, based on Eqs. 1 and 3, when $W/2\ell_S \lesssim 2.7$. This transition is evident in the inset of Fig. 3, where the mobilities have been plotted to emphasize deviations from SD behavior.

Mobility measurements of smectic islands in thin, inclined films extend these rheological investigations into a regime with even larger ε. When the Saffman length ℓ_S is small, as is the case in 8CB films a few (2 – 5) layers thick, air plays an important role in the hydrodynamics of inclusions. This regime was investigated using video microscopy to track the motion of smectic islands of radius a, sketched in Fig. 5a and b, in a circular film of radius $R = 1.5$ mm. The film was inclined by $-15° \lesssim \delta \lesssim 15°$ so that islands of different sizes ($5 < a < 50$ μm) attained easily observable terminal velocities of a few µm/s. The Saffman length in these experiments ($\ell_S \sim 20$ µm) is considerably smaller than R, and the measured mobilities are in good agreement with the extended SD/HPW model (Fig. 5c). Since ℓ_S

is about two orders of magnitude smaller than the film radius in these experiments, contributions to the island mobility from confinement should be negligible. The observations are consistent with an extensive earlier study of the Brownian diffusion of islands in ultra-thin 8CB films, which showed that the islands have mobilities that follow SD/HPW theory over a wide range of ε [7]. Although they have fluid interiors, circulatory flow inside the islands induced by their motion through the background film is expected to be strongly suppressed, so that they behave hydrodynamically like solid discs. This is because the dissipation associated with the permeative flow across an island boundary required to sustain flow in the island interior is three or four orders of magnitude larger than that associated with shear flow around an island with no-slip boundary conditions[13, 14].

In conclusion, we have explored the hydrodynamics of two-dimensional flow by direct measurement of the gravitational motion of small inclusions in inclined smectic-A liquid crystal films. This system allows us to vary characteristic lengthscales over a wide range and access different hydrodynamic regimes in 2D. In films where the Saffman length is comparable to or larger than the film width, the motion of small inclusions ($a \ll \ell_S$) is governed solely by confinement effects. The motion of an embedded bead and the fluid flow in the film are well described in this case by the 2D Navier-Stokes equations neglecting air friction, and the mobility by Eq. 3. Confinement continues to be important up to a crossover to the SD regime, where air-film coupling becomes significant. When the Saffman length is sufficiently small (less than the film width), a condition readily obtained in thin films, the coupling between the air and the fluid flow in the membrane completely determines the dynamic behavior of inclusions. This regime was studied both with beads and using smectic islands, with the measured mobilities confirming the predictions of the SD/HPW model.

This work was supported by DFG Grant STA 424/28-1, BMWT Grant OASIS-CO, NASA Grant NAG-NNX07AE48G, and by NSF MRSEC Grant DMR-0820579.

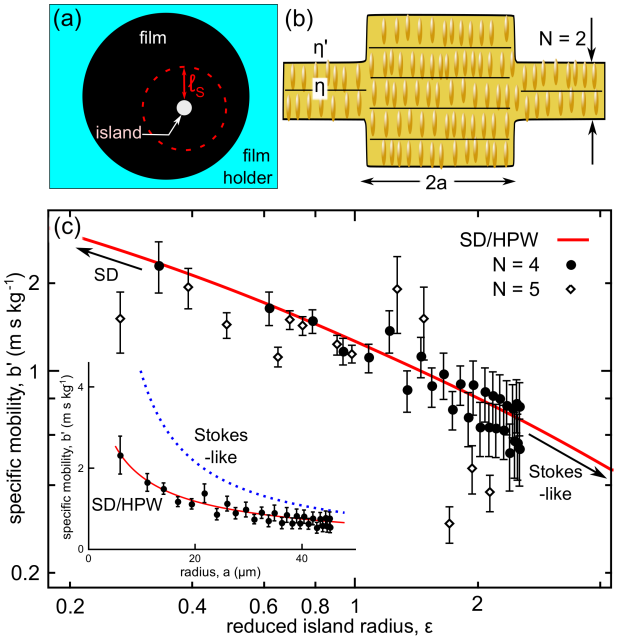

FIG. 5: Mobility of smectic islands in freely-suspended 8CB films. (a) Top view of an island in a thin film. The Saffman region is greatly exaggerated in this illustration, ℓ_S being much smaller than the film radius in these experiments. (b) Side view of a 5-layer island of radius a in an $N = 2$ film. The viscosities of the film and the surrounding fluid (air) are η and η', respectively. (c) Scaled mobility b' as a function of reduced radius ε of a 22-layer island in an $N = 4$ film (•) and of a 13-layer island in an $N = 5$ film (⋄). The mobilities of these islands are around the crossover between the hydrodynamic regime dominated by dissipation in the film due to SD air-film coupling and that dominated by Stokes-like dissipation in the air at even larger $\varepsilon \gg 1$. The mobilities are in qualitative agreement with SD/HPW theory as approximated by Petrov and Schwille [15] (red curve). The number of smectic layers was determined using optical reflectivity and we assumed a smectic layer spacing of $d = 3.17$ nm [16]. The inset shows the scaled mobility of the 22-layer island as a function of island radius a, together with the SD/HPW theory (solid curve) and the Stokes-like prediction for $\varepsilon \gg 1$ (dashed curve). Scatter in the experimental data is due to backlash of the film stage goniometer.

[1] P. G. Saffman and M. Delbrück, Proc. Nat. Acad. Sci. USA **72**, 3111 (1975).
[2] P. G. Saffman, J. Fluid Mech. **73**, 593 (1976).
[3] P. Cicuta, S. Keller, and S. L. Veatch, J. Phys. Chem. B **11**, 3328 (2007).
[4] K. Simons and E. Ikonen, Nature **387**, 569 (1997).
[5] S. Aliaskarisohi, P. Tierno, P. Dhar, Z. Khattari, M. Blaszczynski, and T. Fischer, J. Fluid Mech. **654**, 417 (2010).
[6] V. Prasad and E. R. Weeks, Phys. Rev. E **80**, 026309 (2009).
[7] Z. H. Nguyen, M. Atkinson, C. S. Park, J. Maclennan, M. Glaser, and N. Clark, Phys. Rev. Lett. **105**, 268304 (2010).
[8] C. Cheung, Y. Hwang, and X. Wu, Phys. Rev. Lett. **76**, 2531 (1996).
[9] B. D. Hughes, B. A. Pailthorpe, and L. R. White, J. Fluid Mech. **110**, 349 (2006).
[10] C. Young, R. Pindak, N. A. Clark, and R. B. Meyer, Phys. Rev. Lett. **40**, 773 (1978).
[11] R. Weast (Ed.), *Handbook of Chemistry and Physics - 54th Edition 1973-1974* (CRC Press, 1973).
[12] F. Schneider, Phys. Rev. E **74**, 21709 (2006).
[13] F. Picano, R. Hołyst, and P. Oswald, Phys. Rev. E **62**, 3747 (2000).
[14] P. Oswald and P. Pieranski, *Smectic and Columnar Liquid Crystals* (CRC Press, 2006).
[15] E. P. Petrov and P. Schwille, Biophys J **94**, L41 (2008).

[16] D. Davidov, C. R. Safinya, M. Kaplan, S. S. Dana, R. Schaetzing, R. J. Birgeneau, and J. D. Litster, Phys. Rev. B **19**, 1657 (1979).